

The isotropic relaxed micromorphic model in polar coordinates and its application to an elastostatic axisymmetric extension problem

Esmaeal Ghavanloo¹ and Patrizio Neff²

December 6, 2024

Abstract

In this paper, we consider the isotropic relaxed micromorphic model in polar coordinates and use this representation to solve explicitly an elastostatic axisymmetric extension problem involving a linear system of ordinary differential equations. To obtain an analytical solution, modified Bessel functions are utilized and closed-form solutions for the displacement and microdistortion are obtained. We show how certain limit cases (classical linear elasticity), which are naturally included in the relaxed micromorphic model, can be efficiently achieved. Furthermore, numerical results are calculated and the effects of various parameters are examined. The results can be used to calibrate and check corresponding finite element codes.

Keywords: generalized continua, relaxed micromorphic model, polar coordinates; axisymmetric extension problem; consistent coupling

1 Introduction

Experimental observations in both natural and synthetic materials (e.g., metamaterials) demonstrate that their physical behavior varies with size [6, 19], making it impossible to accurately predict these behaviors using classical continuum theory. To overcome this limitation, various generalized continuum models have been developed, that extend classical continuum theory for modeling size-dependent responses [5, 11]. These generalized continuum models are typically classified into two categories. In the first category, various additional degrees of freedom, such as micro-rotation [17], micro-stretch, and micro-strain [10], are introduced to describe the deformation of the microstructure. The classical micromorphic theory [9, 22] and the Cosserat theory [27] are two of the most well-known theories in this category. The second category of generalized continua involves the incorporation of higher-order differential operators in the energy or motion functional [3]. The strain gradient theory is the most well-known theory within that category [1].

Among the various generalized continuum models, micromorphic models have been particularly successful in describing the behavior of mechanical metamaterials [2], composites [28], porous media [15], and granular materials [41]. However, the classical micromorphic theory involves a large number of material coefficients (18 in the linear-isotropic case), which restricts its practical use. To address these limitations, various simplified versions of the micromorphic theory have been developed over the past decade [24, 33, 38, 42]. The relaxed micromorphic model is a generalized continuum model that effectively describes size effects while significantly reducing the number of material coefficients required compared to the classical theory. Over the past decade, this model has been successfully applied to solve a wide range of static and dynamic problems [14, 16, 20, 26, 30, 31, 32, 39]. The ongoing development and refinement of the relaxed micromorphic model continue to expand its applicability, promising further advancements in the understanding and utilization of complex material systems.

In the relaxed micromorphic model, the kinematics are defined by the classical displacement $u : \Omega \rightarrow \mathbb{R}^3$ and the non-symmetric micro-distortion $P : \Omega \rightarrow \mathbb{R}^{3 \times 3}$. The solution is subsequently obtained from the variational two-field problem [40]:

$$I(u, P) = \int_{\Omega} \frac{1}{2} \left(\langle C_e \operatorname{sym}(Du - P), \operatorname{sym}(Du - P) \rangle + \langle C_c \operatorname{skew}(Du - P), \operatorname{skew}(Du - P) \rangle \right. \\ \left. + \langle C_{\text{micro}} \operatorname{sym} P, \operatorname{sym} P \rangle + \mu_{\text{macro}} L_c^2 \langle \mathbb{L} \operatorname{Curl} P, \operatorname{Curl} P \rangle \right) dx \longrightarrow \min(u, P), \quad (1)$$

¹Corresponding author: Esmaeal Ghavanloo, School of Mechanical Engineering, Shiraz University, Shiraz, 71963-16548, Iran, email: ghavanloo@shirazu.ac.ir

²Patrizio Neff, Head of Chair for Nonlinear Analysis and Modelling, Fakultät für Mathematik, Universität Duisburg-Essen, Thea-Leymann-Straße 9, 45127 Essen, Germany, email: patrizio.neff@uni-due.de

where $\mathbb{C}_e, \mathbb{C}_{\text{micro}}, \mathbb{L}$ are positive-definite fourth-order tensors, \mathbb{C}_c is a positive semi-definite fourth order tensor, L_c is a characteristic length and μ_{macro} is the macroscopic shear modulus added for dimensional consistency. In addition, the stiffness tensors $\mathbb{C}_{\text{macro}}, \mathbb{C}_e$ and $\mathbb{C}_{\text{micro}}$ are related together by the following relationships [4, 24]:

$$\begin{aligned} \mathbb{C}_e = \mathbb{C}_{\text{micro}} \left(\mathbb{C}_{\text{micro}} - \mathbb{C}_{\text{macro}} \right)^{-1} \mathbb{C}_{\text{macro}} &\iff \mathbb{C}_{\text{macro}} = \mathbb{C}_{\text{micro}} \left(\mathbb{C}_{\text{micro}} + \mathbb{C}_e \right)^{-1} \mathbb{C}_e, \\ \mathbb{C}_{\text{micro}} = \mathbb{C}_e \left(\mathbb{C}_e - \mathbb{C}_{\text{macro}} \right)^{-1} \mathbb{C}_{\text{macro}}, & \end{aligned} \quad (2)$$

The original relaxed micromorphic model, along with its derived models, has been formulated in general tensor forms [8]. This formulation allows for theoretical adaptation to specific problems where Cartesian coordinates are suitable. When applying the relaxed micromorphic model in scenarios where curvilinear coordinates (such as polar, cylindrical, or spherical coordinates) are more appropriate, deriving the corresponding formulations for governing equations and boundary conditions is not straightforward. The process is often complex, tedious, and challenging. However, to date, in spite of the vast application of the relaxed micromorphic model in prediction of the mechanical behavior of various natural and man-made materials, its general formulation in orthogonal curvilinear coordinates is absent in the literature. Motivated by this missing development, we derive general formulations for the relaxed micromorphic model in polar coordinates by utilizing the expressions for divergence, curl, and gradient operators of tensors in these coordinates. Then, to demonstrate the practical application of the presented formulation, we analytically solve an elastostatic axisymmetric extension problem. This involves analyzing the deformation of a thin circular plate subjected to uniform radial displacement at its boundary, using modified Bessel's functions. In addition, it is demonstrated that the classical elasticity model can be derived as limit-cases of the relaxed micromorphic solution. Finally, numerical results are calculated to illustrate the effects of various parameters, including material coefficients of the relaxed micromorphic model and the characteristic length.

2 The isotropic relaxed micromorphic model

The isotropic relaxed micromorphic model exhibits the same kinematics as the classical micromorphic isotropic model [9, 22]. In this framework, the displacement u and the non-symmetric microdistortion P are independent fields. The operator form of governing equations of motion in the absence of body forces is given by [21]

$$\rho \ddot{u} = \text{Div } \sigma, \quad \eta \ddot{P} = \sigma - \sigma_{\text{micro}} - \text{Curl } m, \quad (3)$$

where

$$\begin{aligned} \sigma &:= 2\mu_e \text{sym}(Du - P) + 2\mu_c \text{skew}(Du - P) + \lambda_e \text{tr}(Du - P) \mathbb{1}, \\ \sigma_{\text{micro}} &:= 2\mu_{\text{micro}} \text{sym } P + \lambda_{\text{micro}} \text{tr}(P) \mathbb{1}, \\ m &:= \mu_{\text{macro}} L_c^2 \text{Curl } P, \end{aligned} \quad (4)$$

where σ is the non-symmetric elastic force stress tensor, σ_{micro} is the symmetric microscopic stress tensor, m is the non-symmetric moment tensor, ρ and η are the macro and micro mass densities respectively and all other quantities ($\mu_e, \lambda_e, \mu_c, \mu_{\text{micro}}, \lambda_{\text{micro}}, \mu_{\text{macro}}$ and L_c) are the constitutive parameters of the model. Furthermore, $\mathbb{1}$ denotes the identity matrix, Div represents the row-wise divergence operator, D denotes the gradient operator, sym and skew indicate the symmetric and skew-symmetric parts of a tensor, respectively.

The homogeneous Neumann and the Dirichlet boundary conditions are

$$\text{Neumann:} \quad t := \sigma \cdot n = 0, \quad \text{and} \quad \eta := m \times n = 0, \quad (5)$$

$$\text{Dirichlet:} \quad u = \bar{u}, \quad \text{and} \quad \bar{Q} = P \cdot \tau, \quad (6)$$

in which τ and n are the outer tangent and normal vector on the boundary. The higher-order Dirichlet boundary conditions in Eq. (6) can be particularised to [37]

$$P \cdot \tau = \bar{Q} = Du \cdot \tau, \quad (7)$$

called ‘‘consistent coupling boundary conditions’’ [7].

3 The isotropic relaxed micromorphic model in polar coordinates

3.1 Governing equations

In this section, the formulations of the isotropic two-dimensional relaxed micromorphic model in polar coordinates will be derived. In the polar coordinates, the position of a material point is identified by r and θ , where r is the radial distance from the origin and θ is the azimuthal angle. The displacement field u and the micro-distortion tensor P can be expressed in the polar coordinates as follows:

$$u = u_r(r, \theta) \mathbf{e}_r + u_\theta(r, \theta) \mathbf{e}_\theta, \quad (8)$$

$$P = P_{rr}(r, \theta) \mathbf{e}_r \otimes \mathbf{e}_r + P_{r\theta}(r, \theta) \mathbf{e}_r \otimes \mathbf{e}_\theta + P_{\theta r}(r, \theta) \mathbf{e}_\theta \otimes \mathbf{e}_r + P_{\theta\theta}(r, \theta) \mathbf{e}_\theta \otimes \mathbf{e}_\theta, \quad (9)$$

where \mathbf{e}_r and \mathbf{e}_θ are the unit vectors in r and θ directions respectively. Furthermore, u_r and u_θ denote the radial and angular displacements, respectively. To present Eqs. (3-4) in polar coordinates, the gradient of the displacement field, the divergence of the stress tensor, and the curl of the microdistortion tensor must be properly defined in polar coordinates. The gradient of displacement field can be expressed as [34]

$$Du = \frac{\partial u_r}{\partial r} \mathbf{e}_r \otimes \mathbf{e}_r + \frac{1}{r} \left(\frac{\partial u_r}{\partial \theta} - u_\theta \right) \mathbf{e}_r \otimes \mathbf{e}_\theta + \frac{\partial u_\theta}{\partial r} \mathbf{e}_\theta \otimes \mathbf{e}_r + \frac{1}{r} \left(\frac{\partial u_\theta}{\partial \theta} + u_r \right) \mathbf{e}_\theta \otimes \mathbf{e}_\theta. \quad (10)$$

In addition, the divergence of the stress tensor σ can be express as

$$\text{Div } \sigma = \left(\frac{\partial \sigma_{rr}}{\partial r} + \frac{1}{r} \frac{\partial \sigma_{r\theta}}{\partial \theta} + \frac{\sigma_{rr} - \sigma_{\theta\theta}}{r} \right) \mathbf{e}_r + \left(\frac{\partial \sigma_{\theta r}}{\partial r} + \frac{1}{r} \frac{\partial \sigma_{\theta\theta}}{\partial \theta} + \frac{\sigma_{r\theta} + \sigma_{\theta r}}{r} \right) \mathbf{e}_\theta, \quad (11)$$

where σ_{rr} , $\sigma_{r\theta}$, $\sigma_{\theta r}$ and $\sigma_{\theta\theta}$ are the components of the stress tensor.

Now, using Eqs. (3), (4), (9)-(11), we obtain

$$\begin{aligned} \rho \frac{\partial^2 u_r}{\partial t^2} = & \mu_e \left(2 \left[\frac{\partial^2 u_r}{\partial r^2} + \frac{1}{r} \frac{\partial u_r}{\partial r} - \frac{u_r}{r^2} + \frac{P_{\theta\theta} - P_{rr}}{r} - \frac{\partial P_{rr}}{\partial r} \right] + \frac{1}{r^2} \frac{\partial^2 u_r}{\partial \theta^2} - \frac{3}{r^2} \frac{\partial u_\theta}{\partial \theta} + \frac{1}{r} \frac{\partial^2 u_\theta}{\partial r \partial \theta} - \frac{1}{r} \frac{\partial P_{r\theta}}{\partial \theta} - \frac{1}{r} \frac{\partial P_{\theta r}}{\partial \theta} \right) \\ & + \lambda_e \left(\frac{1}{r} \frac{\partial^2 u_\theta}{\partial r \partial \theta} - \frac{\partial P_{\theta\theta}}{\partial r} + \frac{\partial^2 u_r}{\partial r^2} + \frac{1}{r} \frac{\partial u_r}{\partial r} - \frac{u_r}{r^2} - \frac{1}{r^2} \frac{\partial u_\theta}{\partial \theta} - \frac{\partial P_{rr}}{\partial r} \right) \\ & + \mu_c \left(\frac{1}{r^2} \frac{\partial^2 u_r}{\partial \theta^2} - \frac{1}{r^2} \frac{\partial u_\theta}{\partial \theta} - \frac{1}{r} \frac{\partial^2 u_\theta}{\partial r \partial \theta} - \frac{1}{r} \frac{\partial P_{r\theta}}{\partial \theta} + \frac{1}{r} \frac{\partial P_{\theta r}}{\partial \theta} \right), \end{aligned} \quad (12)$$

$$\begin{aligned} \rho \frac{\partial^2 u_\theta}{\partial t^2} = & \mu_e \left(\frac{1}{r} \frac{\partial^2 u_r}{\partial r \partial \theta} + \frac{1}{r^2} \frac{\partial u_r}{\partial \theta} + \frac{2}{r^2} \frac{\partial u_r}{\partial \theta} + \frac{\partial^2 u_\theta}{\partial r^2} + \frac{2}{r^2} \frac{\partial^2 u_\theta}{\partial \theta^2} + \frac{1}{r} \frac{\partial u_\theta}{\partial r} - \frac{u_\theta}{r^2} - \frac{\partial P_{r\theta}}{\partial r} - \frac{\partial P_{\theta r}}{\partial r} - \frac{2}{r} \frac{\partial P_{\theta\theta}}{\partial \theta} - 2 \frac{P_{r\theta} + P_{\theta r}}{r} \right) \\ & + \lambda_e \left(\frac{1}{r} \frac{\partial^2 u_r}{\partial r \partial \theta} + \frac{1}{r^2} \frac{\partial^2 u_\theta}{\partial \theta^2} + \frac{1}{r^2} \frac{\partial u_r}{\partial \theta} - \frac{1}{r} \frac{\partial P_{rr}}{\partial \theta} - \frac{1}{r} \frac{\partial P_{\theta\theta}}{\partial \theta} \right) \\ & + \mu_c \left(\frac{1}{r^2} \frac{\partial u_r}{\partial \theta} - \frac{u_\theta}{r^2} - \frac{1}{r} \frac{\partial^2 u_r}{\partial r \partial \theta} + \frac{1}{r} \frac{\partial u_\theta}{\partial r} + \frac{\partial^2 u_\theta}{\partial r^2} - \frac{\partial P_{\theta r}}{\partial r} + \frac{\partial P_{r\theta}}{\partial r} \right). \end{aligned} \quad (13)$$

In addition, the Curl of the micro-distortion tensor can be written as [29]

$$\text{Curl } P = \left(\frac{\partial P_{\theta r}}{\partial r} - \frac{1}{r} \frac{\partial P_{rr}}{\partial \theta} + \frac{1}{r} (P_{r\theta} + P_{\theta r}) \right) \mathbf{e}_z \otimes \mathbf{e}_r + \left(\frac{\partial P_{\theta\theta}}{\partial r} + \frac{P_{\theta\theta} - P_{rr}}{r} - \frac{1}{r} \frac{\partial P_{r\theta}}{\partial \theta} \right) \mathbf{e}_z \otimes \mathbf{e}_\theta, \quad (14)$$

in which \mathbf{e}_z denotes the unit vector normal to the $r - \theta$ plane. As a result, using Eqs. (4) and (14), the nonsymmetric moment tensor m is obtained as

$$\begin{aligned} m = & m_{zr} \mathbf{e}_z \otimes \mathbf{e}_r + m_{z\theta} \mathbf{e}_z \otimes \mathbf{e}_\theta \\ = & \mu_{\text{macro}} L_c^2 \left(\frac{\partial P_{\theta r}}{\partial r} - \frac{1}{r} \frac{\partial P_{rr}}{\partial \theta} + \frac{1}{r} (P_{r\theta} + P_{\theta r}) \right) \mathbf{e}_z \otimes \mathbf{e}_r + \mu_{\text{macro}} L_c^2 \left(\frac{\partial P_{\theta\theta}}{\partial r} + \frac{P_{\theta\theta} - P_{rr}}{r} - \frac{1}{r} \frac{\partial P_{r\theta}}{\partial \theta} \right) \mathbf{e}_z \otimes \mathbf{e}_\theta. \end{aligned} \quad (15)$$

Furthermore, the Curl of m is derived as

$$\begin{aligned} \frac{1}{\mu_{\text{macro}} L_c^2} \text{Curl } m = & \frac{1}{\mu_{\text{macro}} L_c^2} \left[\left(\frac{1}{r} \frac{\partial m_{zr}}{\partial \theta} - \frac{m_{z\theta}}{r} \right) \mathbf{e}_r \otimes \mathbf{e}_r - \left(\frac{\partial m_{z\theta}}{\partial r} \right) \mathbf{e}_\theta \otimes \mathbf{e}_\theta \right. \\ & \left. + \left(\frac{1}{r} \frac{\partial m_{z\theta}}{\partial \theta} + \frac{m_{zr}}{r} \right) \mathbf{e}_r \otimes \mathbf{e}_\theta - \left(\frac{\partial m_{zr}}{\partial r} \right) \mathbf{e}_\theta \otimes \mathbf{e}_r \right] \\ = & \left(\frac{1}{r} \frac{\partial^2 P_{\theta r}}{\partial r \partial \theta} - \frac{1}{r^2} \frac{\partial^2 P_{rr}}{\partial \theta^2} + \frac{1}{r^2} \frac{\partial P_{\theta r}}{\partial \theta} - \frac{1}{r} \frac{\partial P_{\theta\theta}}{\partial r} - \frac{P_{\theta\theta} - P_{rr}}{r^2} + \frac{2}{r^2} \frac{\partial P_{r\theta}}{\partial \theta} \right) \mathbf{e}_r \otimes \mathbf{e}_r \end{aligned} \quad (16)$$

$$\begin{aligned}
& + \left(\frac{1}{r} \frac{\partial^2 P_{\theta\theta}}{\partial r \partial \theta} + \frac{1}{r^2} \frac{\partial P_{\theta\theta}}{\partial \theta} - \frac{2}{r^2} \frac{\partial P_{rr}}{\partial \theta} - \frac{1}{r^2} \frac{\partial^2 P_{r\theta}}{\partial \theta^2} + \frac{1}{r} \frac{\partial P_{\theta r}}{\partial r} + \frac{P_{r\theta} + P_{\theta r}}{r^2} \right) \mathbf{e}_r \otimes \mathbf{e}_\theta \\
& + \left(-\frac{\partial^2 P_{\theta r}}{\partial r^2} - \frac{1}{r^2} \frac{\partial P_{rr}}{\partial \theta} + \frac{1}{r} \frac{\partial^2 P_{rr}}{\partial r \partial \theta} + \frac{P_{r\theta} + P_{\theta r}}{r^2} - \frac{1}{r} \frac{\partial P_{r\theta}}{\partial r} - \frac{1}{r} \frac{\partial P_{\theta r}}{\partial r} \right) \mathbf{e}_\theta \otimes \mathbf{e}_r \\
& + \left(-\frac{\partial^2 P_{\theta\theta}}{\partial r^2} + \frac{P_{\theta\theta} - P_{rr}}{r^2} - \frac{1}{r} \frac{\partial P_{\theta\theta}}{\partial r} + \frac{1}{r} \frac{\partial P_{rr}}{\partial r} - \frac{1}{r^2} \frac{\partial P_{r\theta}}{\partial \theta} + \frac{1}{r} \frac{\partial^2 P_{r\theta}}{\partial r \partial \theta} \right) \mathbf{e}_\theta \otimes \mathbf{e}_\theta.
\end{aligned}$$

Substituting Eqs. (4), (9), (10), and (15) in Eq. (3), yields

$$\begin{aligned}
\eta \frac{\partial^2 P_{rr}}{\partial t^2} &= 2\mu_e \left(\frac{\partial u_r}{\partial r} - P_{rr} \right) + \lambda_e \left(\frac{\partial u_r}{\partial r} + \frac{1}{r} \left(\frac{\partial u_\theta}{\partial \theta} + u_r \right) - (P_{rr} + P_{\theta\theta}) \right) \\
& - 2\mu_{\text{micro}} P_{rr} - \lambda_{\text{micro}} (P_{rr} + P_{\theta\theta}) \\
& - \mu_{\text{macro}} L_c^2 \left(\frac{1}{r} \frac{\partial^2 P_{\theta r}}{\partial r \partial \theta} - \frac{1}{r^2} \frac{\partial^2 P_{rr}}{\partial \theta^2} + \frac{1}{r^2} \frac{\partial P_{\theta r}}{\partial \theta} - \frac{1}{r} \frac{\partial P_{\theta\theta}}{\partial r} - \frac{P_{\theta\theta} - P_{rr}}{r^2} + \frac{2}{r^2} \frac{\partial P_{r\theta}}{\partial \theta} \right), \quad (17)
\end{aligned}$$

$$\begin{aligned}
\eta \frac{\partial^2 P_{r\theta}}{\partial t^2} &= 2\mu_e \left(\frac{1}{2r} \left(\frac{\partial u_r}{\partial \theta} - u_\theta \right) + \frac{1}{2} \frac{\partial u_\theta}{\partial r} - \frac{P_{r\theta} + P_{\theta r}}{2} \right) \\
& - \mu_{\text{micro}} (P_{r\theta} + P_{\theta r}) + 2\mu_c \left(\frac{1}{2r} \left(\frac{\partial u_r}{\partial \theta} - u_\theta \right) - \frac{1}{2} \frac{\partial u_\theta}{\partial r} - \frac{P_{r\theta} - P_{\theta r}}{2} \right) \\
& - \mu_{\text{macro}} L_c^2 \left(\frac{1}{r} \frac{\partial^2 P_{\theta\theta}}{\partial r \partial \theta} + \frac{1}{r^2} \frac{\partial P_{\theta\theta}}{\partial \theta} - \frac{2}{r^2} \frac{\partial P_{rr}}{\partial \theta} - \frac{1}{r^2} \frac{\partial^2 P_{r\theta}}{\partial \theta^2} + \frac{1}{r} \frac{\partial P_{\theta r}}{\partial r} + \frac{P_{r\theta} + P_{\theta r}}{r^2} \right), \quad (18)
\end{aligned}$$

$$\begin{aligned}
\eta \frac{\partial^2 P_{\theta r}}{\partial t^2} &= 2\mu_e \left(\frac{1}{2r} \left(\frac{\partial u_r}{\partial \theta} - u_\theta \right) + \frac{1}{2} \frac{\partial u_\theta}{\partial r} - \frac{P_{r\theta} + P_{\theta r}}{2} \right) \\
& - \mu_{\text{micro}} (P_{r\theta} + P_{\theta r}) + 2\mu_c \left(-\frac{1}{2r} \left(\frac{\partial u_r}{\partial \theta} - u_\theta \right) + \frac{1}{2} \frac{\partial u_\theta}{\partial r} - \frac{P_{\theta r} - P_{r\theta}}{2} \right) \\
& - \mu_{\text{macro}} L_c^2 \left(-\frac{\partial^2 P_{\theta r}}{\partial r^2} - \frac{1}{r^2} \frac{\partial P_{rr}}{\partial \theta} + \frac{1}{r} \frac{\partial^2 P_{rr}}{\partial r \partial \theta} + \frac{P_{r\theta} + P_{\theta r}}{r^2} - \frac{1}{r} \frac{\partial P_{r\theta}}{\partial r} - \frac{1}{r} \frac{\partial P_{\theta r}}{\partial r} \right), \quad (19)
\end{aligned}$$

$$\begin{aligned}
\eta \frac{\partial^2 P_{\theta\theta}}{\partial t^2} &= 2\mu_e \left(\frac{1}{r} \left(\frac{\partial u_\theta}{\partial \theta} + u_r \right) - P_{\theta\theta} \right) + \lambda_e \left(\frac{\partial u_r}{\partial r} + \frac{1}{r} \left(\frac{\partial u_\theta}{\partial \theta} + u_r \right) - (P_{rr} + P_{\theta\theta}) \right) \\
& - 2\mu_{\text{micro}} P_{\theta\theta} - \lambda_{\text{micro}} (P_{rr} + P_{\theta\theta}) \\
& - \mu_{\text{macro}} L_c^2 \left(-\frac{\partial^2 P_{\theta\theta}}{\partial r^2} + \frac{P_{\theta\theta} - P_{rr}}{r^2} - \frac{1}{r} \frac{\partial P_{\theta\theta}}{\partial r} + \frac{1}{r} \frac{\partial P_{rr}}{\partial r} - \frac{1}{r^2} \frac{\partial P_{r\theta}}{\partial \theta} + \frac{1}{r} \frac{\partial^2 P_{r\theta}}{\partial r \partial \theta} \right). \quad (20)
\end{aligned}$$

3.2 Consistent coupling boundary conditions in polar coordinates

Boundary conditions are an essential part of any model formulation. For classical linear elasticity, we typically have either Dirichlet and Neumann conditions on the displacement or stress, respectively. One of the challenges in generalized continua is the inclusion of additional degrees of freedom. For them, the interpretation and adequacy of boundary conditions is an ongoing field of research [7]. From the physical perspective, if one prefers to understand the microdistortion P , it is considered necessary to prescribe the full Dirichlet condition at the boundary. However, in the relaxed micromorphic model, this is not possible because only the curl of P is controlled within the energy function. Therefore, one only needs to prescribe the tangential traces of P at the boundary. However, it is not clear at all if $P \cdot \tau$ should be set to zero. That the tangential traces of P need to be prescribed is evident from the mathematical existence theories based on the incompatible Korn's inequality [12, 13, 18, 25]. Neff and co-workers [7] have observed that at the Dirichlet part of the boundary, where the displacement u is prescribed, there is also an additional prescribed tangential part of $Du \cdot \tau$. The idea of the consistent coupling boundary condition is to set $P \cdot \tau = Du \cdot \tau$ on the boundary. Since $\text{Curl}(Du - P) = -\text{Curl}(P)$, the combination $(Du - P)$ indeed has tangential traces at the boundary.

Here, we rewrite the consistent coupling condition in polar coordinates for the general case. In this context, $\tau = \tau_r \mathbf{e}_r + \tau_\theta \mathbf{e}_\theta$, and applying Eqs. (9) and (10) yields

$$P \cdot \tau = (P_{rr}\tau_r + P_{r\theta}\tau_\theta) \mathbf{e}_r + (P_{\theta r}\tau_r + P_{\theta\theta}\tau_\theta) \mathbf{e}_\theta, \quad (21)$$

$$Du \cdot \tau = \left(\frac{\partial u_r}{\partial r} \tau_r + \frac{1}{r} \left(\frac{\partial u_r}{\partial \theta} - u_\theta \right) \tau_\theta \right) \mathbf{e}_r + \left(\frac{\partial u_\theta}{\partial r} \tau_r + \frac{1}{r} \left(\frac{\partial u_\theta}{\partial \theta} + u_r \right) \tau_\theta \right) \mathbf{e}_\theta. \quad (22)$$

By substituting Eqs. (21) and (22) into $P \cdot \tau = Du \cdot \tau$ at the boundary of the domain, we derive the following result:

$$P_{rr}\tau_r + P_{r\theta}\tau_\theta = \frac{\partial u_r}{\partial r}\tau_r + \frac{1}{r}\left(\frac{\partial u_r}{\partial \theta} - u_\theta\right)\tau_\theta, \quad (23)$$

$$P_{\theta r}\tau_r + P_{\theta\theta}\tau_\theta = \frac{\partial u_\theta}{\partial r}\tau_r + \frac{1}{r}\left(\frac{\partial u_\theta}{\partial \theta} + u_r\right)\tau_\theta. \quad (24)$$

If the boundary is circular with radius R , we have $\tau = \mathbf{e}_\theta$. Therefore, $\tau_r = 0$ and $\tau_\theta = 1$, leading to the following result:

$$P \cdot \tau = P_{r\theta} \mathbf{e}_r + P_{\theta\theta} \mathbf{e}_\theta, \quad (25)$$

$$Du \cdot \tau = \frac{1}{r}\left(\frac{\partial u_r}{\partial \theta} - u_\theta\right) \mathbf{e}_r + \frac{1}{r}\left(\frac{\partial u_\theta}{\partial \theta} + u_r\right) \mathbf{e}_\theta. \quad (26)$$

Equating Eqs. (25) and (26), we obtain

$$P_{r\theta}(R) = \frac{1}{R}\left(\frac{\partial u_r(R)}{\partial \theta} - u_\theta(R)\right), \quad (27)$$

$$P_{\theta\theta}(R) = \frac{1}{R}\left(\frac{\partial u_\theta(R)}{\partial \theta} + u_r(R)\right). \quad (28)$$

4 Elastostatic axisymmetric extension problem

4.1 Formulations and solution method

Here, we consider an elastostatic axisymmetric extension problem that involves analyzing the deformation of a long circular cylinder with radius R under the influence of uniform radial displacement at the boundary (see Figure 1). In this special case, both the displacement field and the micro-distortion tensor depend solely on the radial coordinate ($u_r(r)$, $P_{rr}(r)$, $P_{\theta\theta}(r)$, $P_{r\theta}(r)$ and $P_{\theta r}(r)$), and we have also $u_\theta = 0$. By dropping the time-dependent terms and using the mentioned assumptions, the governing equations are simplified as follows:

$$(2\mu_e + \lambda_e)\frac{d}{dr}\left(\frac{du_r}{dr} - P_{rr}\right) + \lambda_e\frac{d}{dr}\left(\frac{u_r}{r} - P_{\theta\theta}\right) = -2\mu_e\frac{d}{dr}\left(\frac{u_r}{r} - P_{\theta\theta}\right) - 2\mu_e\left(\frac{dP_{\theta\theta}}{dr} + \frac{P_{\theta\theta} - P_{rr}}{r}\right), \quad (29)$$

$$\mu_e\left(\frac{dP_{r\theta}}{dr} + \frac{dP_{\theta r}}{dr} + 2\frac{P_{r\theta} + P_{\theta r}}{r}\right) = \mu_c\left(\frac{dP_{r\theta}}{dr} - \frac{dP_{\theta r}}{dr}\right), \quad (30)$$

$$(2\mu_e + \lambda_e)\left(\frac{du_r}{dr} - P_{rr}\right) + \lambda_e\left(\frac{u_r}{r} - P_{\theta\theta}\right) = 2\mu_{\text{micro}}P_{rr} + \lambda_{\text{micro}}(P_{rr} + P_{\theta\theta}) - \frac{\mu_{\text{macro}}L_c^2}{r}\left(\frac{dP_{\theta\theta}}{dr} + \frac{P_{\theta\theta} - P_{rr}}{r}\right), \quad (31)$$

$$\mu_e(P_{r\theta} + P_{\theta r}) + \mu_{\text{micro}}(P_{r\theta} + P_{\theta r}) + \mu_c(P_{r\theta} - P_{\theta r}) + \mu_{\text{macro}}L_c^2\left(\frac{1}{r}\frac{dP_{\theta r}}{dr} + \frac{P_{r\theta} + P_{\theta r}}{r^2}\right) = 0, \quad (32)$$

$$\mu_e(P_{r\theta} + P_{\theta r}) + \mu_{\text{micro}}(P_{r\theta} + P_{\theta r}) + \mu_c(P_{\theta r} - P_{r\theta}) + \mu_{\text{macro}}L_c^2\left(-\frac{d^2P_{\theta r}}{dr^2} + \frac{P_{r\theta} + P_{\theta r}}{r^2} - \frac{1}{r}\frac{dP_{r\theta}}{dr} - \frac{1}{r}\frac{dP_{\theta r}}{dr}\right) = 0, \quad (33)$$

$$(2\mu_e + \lambda_e)\left(\frac{u_r}{r} - P_{\theta\theta}\right) + \lambda_e\left(\frac{du_r}{dr} - P_{rr}\right) = 2\mu_{\text{micro}}P_{\theta\theta} + \lambda_{\text{micro}}(P_{rr} + P_{\theta\theta}) - \mu_{\text{macro}}L_c^2\frac{d}{dr}\left(\frac{dP_{\theta\theta}}{dr} + \frac{P_{\theta\theta} - P_{rr}}{r}\right). \quad (34)$$

The Dirichlet boundary conditions for the axisymmetric extension is

$$u_r(R) = U_0. \quad (35)$$

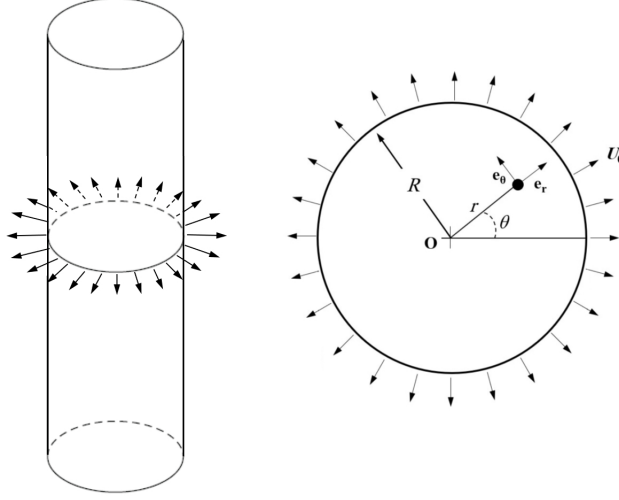


Figure 1: Cross-section of the long circular cylinder with radius R under the influence of uniform radial displacement U_0 . Due to the length of the cylinder, plane-strain conditions are warranted.

Furthermore, using Eqs. (27) and (28), the consistent coupling boundary conditions for the axisymmetric problem are as follows:

$$P_{r\theta}(R) = 0, \quad P_{\theta\theta}(R) = \frac{U_0}{R}. \quad (36)$$

To enhance readability, in the following, we utilize the shortened forms: $\mu_M \equiv \mu_{\text{macro}}$, $\mu_m \equiv \mu_{\text{micro}}$, $\lambda_m \equiv \lambda_{\text{micro}}$ and $\lambda_M \equiv \lambda_{\text{macro}}$. Since the cylinder is long, the plane-strain conditions are warranted. In the context of plane-strain conditions, the bulk micro-moduli κ_e and $\kappa_m \equiv \kappa_{\text{micro}}$ are connected to their corresponding Lamé-type micro-moduli via the two-dimensional relationships [14]:

$$\kappa_e := \lambda_e + \mu_e, \quad \kappa_m := \lambda_m + \mu_m. \quad (37)$$

Accordingly, the relations between the macro moduli ($\mu_M, \lambda_M, \kappa_M$) and the micro-moduli in the plane strain case become [23]

$$\begin{aligned} \mu_M &:= \frac{\mu_e \mu_m}{\mu_e + \mu_m} & \Leftrightarrow & \quad \frac{1}{\mu_M} = \frac{1}{\mu_e} + \frac{1}{\mu_m}, \\ \kappa_M &:= \frac{\kappa_e \kappa_m}{\kappa_e + \kappa_m} & \Leftrightarrow & \quad \frac{1}{\kappa_M} = \frac{1}{\kappa_e} + \frac{1}{\kappa_m}, \\ \lambda_m &:= \frac{(\mu_e + \lambda_e)(\mu_m + \lambda_m)}{(\mu_e + \lambda_e) + (\mu_m + \lambda_m)} - \frac{\mu_e \mu_m}{\mu_e + \mu_m}, \end{aligned} \quad (38)$$

where $\kappa_M \equiv \kappa_{\text{macro}}$ with $\kappa_M = \mu_M + \lambda_M$. To obtain the analytical solution for the problem, it is essential to reformulate the system (29)-(34). First, Eq. (29) is rearranged as follows:

$$(2\mu_e + \lambda_e) \frac{d}{dr} \left(\frac{du_r}{dr} + \frac{u_r}{r} \right) - 2\mu_e \left(\frac{dP_{rr}}{dr} - \frac{P_{\theta\theta} - P_{rr}}{r} \right) - \lambda_e \frac{d}{dr} (P_{\theta\theta} + P_{rr}) = 0. \quad (39)$$

Then, by differentiating Eq. (31) with respect to r , and using Eqs. (29) and (34) along with the simplification, the resultant equation is obtained as:

$$2\mu_m \left(\frac{dP_{rr}}{dr} + \frac{P_{rr} - P_{\theta\theta}}{r} \right) + \lambda_m \frac{d}{dr} (P_{\theta\theta} + P_{rr}) = 0. \quad (40)$$

Substituting Eq. (40) into Eq. (39) yields

$$\frac{du_r}{dr} + \frac{u_r}{r} = \frac{\mu_m \lambda_e - \mu_e \lambda_m}{\mu_m (\mu_e + \kappa_e)} (P_{\theta\theta} + P_{rr}) + C_1, \quad (41)$$

where C_1 is an integration constant. In addition, by summing Eqs. (31) and (34) we have

$$2(\mu_e + \lambda_e) \left(\frac{du_r}{dr} + \frac{u_r}{r} \right) = 2(\kappa_m + \kappa_e)(P_{rr} + P_{\theta\theta}) - \mu_M L_c^2 \frac{d}{dr} \left(\frac{dP_{\theta\theta}}{dr} + \frac{P_{\theta\theta} - P_{rr}}{r} \right) - \mu_M L_c^2 \frac{1}{r} \left(\frac{dP_{\theta\theta}}{dr} + \frac{P_{\theta\theta} - P_{rr}}{r} \right). \quad (42)$$

Now, we define the following variables:

$$X = \frac{du_r}{dr} - P_{rr}, \quad Y = \frac{u_r}{r} - P_{\theta\theta}, \quad Z = P_{\theta\theta} + P_{rr}. \quad (43)$$

Substituting Eq. (43) into Eqs. (40)-(42), we obtain

$$\frac{dY}{dr} + \frac{Y - X}{r} = - \left(\frac{\kappa_m + \mu_m}{2\mu_m} \right) \frac{dZ}{dr}, \quad (44)$$

$$X + Y = - \frac{\mu_e(\kappa_m + \mu_m)}{\mu_m(\kappa_e + \mu_e)} Z + C_1, \quad (45)$$

$$X + Y = \frac{\kappa_m}{\kappa_e} Z + \frac{\mu_M L_c^2}{2\kappa_e} \frac{d}{dr} \left(\frac{dY}{dr} + \frac{Y - X}{r} \right) + \frac{\mu_M L_c^2}{2\kappa_e} \frac{1}{r} \left(\frac{dY}{dr} + \frac{Y - X}{r} \right). \quad (46)$$

By using Eqs. (44) and (45) and simplifying the equations, Eq. (46) can be rewritten as

$$\frac{d^2 Z}{dr^2} + \frac{1}{r} \frac{dZ}{dr} - aZ + b = 0, \quad (47)$$

where

$$a = \frac{4}{\mu_M L_c^2} \left(\frac{\mu_e \kappa_e}{\kappa_e + \mu_e} + \frac{\mu_m \kappa_m}{\kappa_m + \mu_m} \right), \quad b = \frac{4}{\mu_M L_c^2} \frac{C_1 \kappa_e \mu_m}{\kappa_m + \mu_m}. \quad (48)$$

The general solution of Eq. (47) is given by

$$Z(r) = \frac{b}{a} + D_1 I_0(\sqrt{ar}) + D_2 K_0(\sqrt{ar}), \quad (49)$$

where D_1 and D_2 are unknown constants, and I_0 and K_0 are modified Bessel functions of the first and second kind, respectively, of order zero. To ensure the solution remains finite at the center of the plate, D_2 must be set to 0 to eliminate the infinite value of K_0 when $r = 0$. As a result, the solution becomes

$$Z(r) = \frac{b}{a} + D_1 I_0(\sqrt{ar}). \quad (50)$$

Using Eq. (43) and (50), Eq. (41) can be rewritten as

$$\frac{du_r}{dr} + \frac{u_r}{r} = C_1 A + D_1 B I_0(\sqrt{ar}), \quad (51)$$

where now

$$A = 1 + \frac{(\mu_m \lambda_e - \mu_e \lambda_m) \kappa_e}{\mu_e(\kappa_m + \mu_m) \kappa_e + \mu_m(\kappa_e + \mu_e) \kappa_m}, \quad B = \frac{\mu_m \lambda_e - \mu_e \lambda_m}{\mu_m(\mu_e + \kappa_e)}. \quad (52)$$

The general solution of Eq. (51) is obtained by

$$u_r(r) = \frac{C_1 A r}{2} + \frac{D_1 B}{\sqrt{a}} I_1(\sqrt{ar}) + \frac{C_2}{r}, \quad (53)$$

in which C_2 is an integration constant and needs to be set to zero to keep the displacement finite at the center. Furthermore, I_1 is a modified Bessel function of the first kind with order 1. By substituting the boundary condition (35) into Eq. (53), the following relation can be obtained:

$$\frac{C_1 A R}{2} + \frac{D_1 B}{\sqrt{a}} I_1(\sqrt{a}R) = U_0. \quad (54)$$

This equation contains two unknown parameters, C_1 and D_1 . Consequently, an additional boundary condition must be specified from the consistent coupling boundary condition (36). To obtain closed-form expressions for the non-zero components of the microdistortion tensor P , Eqs. (44) and (45) are summed together. The resultant equation is

$$\frac{dY}{dr} + \frac{2Y}{r} = - \left(\frac{\kappa_m + \mu_m}{2\mu_m} \right) \frac{dZ}{dr} - \frac{\mu_e(\kappa_m + \mu_m)}{\mu_m(\kappa_e + \mu_e)} \frac{Z}{r} + \frac{C_1}{r}. \quad (55)$$

Substituting Eq. (50) in Eq. (55) yields

$$\frac{dY}{dr} + \frac{2Y}{r} = D_1 \xi_1 \sqrt{a} I_1(\sqrt{ar}) + D_1 \xi_2 \left(\frac{I_0(\sqrt{ar})}{r} \right) + \frac{C_1 \xi_3}{r}, \quad (56)$$

where

$$\xi_1 = - \frac{(\kappa_m + \mu_m)}{2\mu_m}, \quad \xi_2 = - \frac{\mu_e(\kappa_m + \mu_m)}{\mu_m(\kappa_e + \mu_e)}, \quad \xi_3 = \frac{\kappa_m \mu_m (\kappa_e + \mu_e)}{\kappa_e \mu_e (\kappa_m + \mu_m) + \kappa_m \mu_m (\kappa_e + \mu_e)}. \quad (57)$$

The solution of Eq. (56) is

$$Y = D_1 \xi_1 I_0(\sqrt{ar}) - \frac{D_1 I_1(\sqrt{ar})}{\sqrt{ar}} (2\xi_1 - \xi_2) + \frac{C_1 \xi_3}{2} + \frac{C_3}{r^2}, \quad (58)$$

where C_3 is an integration constant that must be set to zero in order to ensure that Y remains finite at the center. Now, using boundary conditions (35) and (36) and Eq. (43), we obtain

$$Y(R) = 0, \quad (59)$$

Using Eqs. (59) and (58), this leads to:

$$D_1 \left(\xi_1 I_0(\sqrt{aR}) - \frac{I_1(\sqrt{aR})}{\sqrt{aR}} (2\xi_1 - \xi_2) \right) + \frac{C_1 \xi_3}{2} = 0. \quad (60)$$

The two unknown constants C_1 and D_1 are obtained by simultaneously solving Eqs. (54) and (60), as follows:

$$C_1 = \frac{2U_0}{R} \frac{I_1(\sqrt{aR}) (2\xi_1 - \xi_2) - \xi_1 \sqrt{aR} I_0(\sqrt{aR})}{A (I_1(\sqrt{aR}) (2\xi_1 - \xi_2) - \xi_1 \sqrt{aR} I_0(\sqrt{aR})) + B \xi_3 I_1(\sqrt{aR})}, \quad (61)$$

$$D_1 = \frac{U_0 \xi_3 \sqrt{a}}{A (I_1(\sqrt{aR}) (2\xi_1 - \xi_2) - \xi_1 \sqrt{aR} I_0(\sqrt{aR})) + \xi_3 B I_1(\sqrt{aR})}. \quad (62)$$

To complete the solution procedure, it is essential to derive relations for $P_{r\theta}$ and $P_{\theta r}$. In this context, subtracting Eqs. (34) from (33) yields:

$$2\mu_c (P_{r\theta} - P_{\theta r}) = -\frac{\mu_M L_c^2}{r} \left(\frac{d}{dr} \left(r \frac{dP_{\theta r}}{dr} + P_{\theta r} + P_{r\theta} \right) \right). \quad (63)$$

By utilizing Eqs. (30) and (33), Eq. (63) can be rearranged as follows:

$$\frac{d}{dr} (P_{r\theta} + P_{\theta r}) + 2 \left(\frac{P_{r\theta} + P_{\theta r}}{r} \right) = 0. \quad (64)$$

The solution of Eq. (64) is

$$P_{r\theta} + P_{\theta r} = \frac{C_4}{r^2}. \quad (65)$$

To ensure the solution remains finite at $r = 0$, C_4 must be set to 0 and so we have

$$P_{r\theta} = -P_{\theta r}. \quad (66)$$

Substituting Eq. (66) into Eq. (30) yields:

$$\frac{dP_{r\theta}}{dr} = 0. \quad (67)$$

Equation (67) shows that $P_{r\theta} = C_5$ where C_5 is integration constant. By applying the consistent coupling boundary conditions ($P_{r\theta}(R) = 0$), we find $P_{r\theta} = P_{\theta r} = 0$. Finally, it should be noted that, in the case of the axisymmetric problem, the terms involving the Cosserat couple modulus μ_c become zero. As a result, μ_c does not appear in the solution.

Finally, the closed-form expressions for u_r , $P_{\theta\theta}$ and P_{rr} are summarized as follows:

$$u_r(r) = \frac{U_0}{R} \frac{Ar (I_1(\sqrt{aR}) (2\xi_1 - \xi_2) - \xi_1 \sqrt{aR} I_0(\sqrt{aR})) + B \xi_3 R I_1(\sqrt{aR})}{A (I_1(\sqrt{aR}) (2\xi_1 - \xi_2) - \xi_1 \sqrt{aR} I_0(\sqrt{aR})) + B \xi_3 I_1(\sqrt{aR})}, \quad (68)$$

$$P_{\theta\theta} = \frac{C_1}{2} (A - \xi_3) - D_1 \xi_1 I_0(\sqrt{ar}) + \frac{D_1 I_1(\sqrt{ar})}{\sqrt{ar}} (B + 2\xi_1 - \xi_2), \quad (69)$$

$$P_{rr} = Z - P_{\theta\theta}. \quad (70)$$

where A is defined in Eq. (52), Z in Eq. (50), and ξ_1 , ξ_2 , and ξ_3 are given in Eq. (57).

4.2 Limit-cases

In this section, the limit-cases for the relaxed micromorphic model will be explored, particularly its behavior as $0 \leftarrow L_c \rightarrow \infty$. One of the simple cases occurs when both the micro and macro Poisson's ratios are zero, resulting in $\lambda_e = \lambda_m = 0$, which implies that $\lambda_M = 0$. In this case, we have

$$\begin{aligned} u_r(r) &= U_0 \frac{r}{R}, \\ P_{\theta\theta}(r) &= \frac{U_0}{R} (1 - \xi_3) + \left(\frac{\sqrt{ar}I_0(\sqrt{ar}) - I_1(\sqrt{ar})}{\sqrt{aR}I_0(\sqrt{aR}) - I_1(\sqrt{aR})} \right) \frac{U_0 \xi_3}{r}, \\ P_{rr}(r) &= \frac{U_0}{R} \left(\frac{2\kappa_e \mu_m (\mu_e + \kappa_e)}{\mu_e \kappa_e (\mu_m + \kappa_m) + \mu_m \kappa_m (\mu_e + \kappa_e)} + \frac{\xi_3 \sqrt{aR} I_0(\sqrt{ar})}{\sqrt{aR} I_0(\sqrt{aR}) - I_1(\sqrt{aR})} \right) - P_{\theta\theta}, \end{aligned} \quad (71)$$

where

$$a = \frac{2}{L_c^2} \frac{(\mu_e + \mu_m)^2}{\mu_e \mu_m}, \quad \xi_3 = \frac{\mu_m}{\mu_e + \mu_m}. \quad (72)$$

Next, we examine two limit-cases related to classical linear elasticity. In the first scenario, it is assumed that $L_c \rightarrow 0$ represents the lower bound of macroscopic stiffness. As $L_c \rightarrow 0$, we obtain

$$u_r(r) = U_0 \frac{r}{R}, \quad P_{\theta\theta}(r) = \frac{U_0}{R}, \quad P_{rr}(r) = \frac{\kappa_e \mu_E (\mu_e + \kappa_e)}{\mu_e \kappa_e (\mu_m + \kappa_m) + \mu_m \kappa_m (\mu_e + \kappa_e)} \frac{2}{A} \frac{U_0}{R} - \frac{U_0}{R}. \quad (73)$$

In the second case, as L_c approaches infinity, the relaxed micromorphic solution degenerates again to the known classical solution [34]

$$u_r(r) = U_0 \frac{r}{R}, \quad P_{\theta\theta} = \frac{U_0}{R}, \quad P_{rr}(r) = \left(\frac{\kappa_e \mu_m (\mu_e + \kappa_e)}{\mu_e \kappa_e (\mu_m + \kappa_m) + \mu_m \kappa_m (\mu_e + \kappa_e)} (\xi_2 - \xi_3) \right) \frac{2U_0}{(A\xi_2 - B\xi_3)R} - \frac{U_0}{R}. \quad (74)$$

4.3 Numerical results and discussion

In this section, we present numerical results to demonstrate the effects of various parameters, including the material coefficients and the characteristic length. First, variations of the non-dimensional radial displacement as a function of radial position are plotted in Figure 2 for three parameter sets as listed in Table 1, taken from Ref. [35, 36], with $R/L_c = 2$. The figure shows that the non-dimensional radial displacement increases nearly linearly with the radial position for all parameter sets. Furthermore, it is observed that the classical linear elasticity solution coincides with the data from parameter set 1. The reason for this is that in the parameters of set 1, the λ_m and μ_m are proportional to the macro parameters. As a result, $\lambda_e \mu_m = \lambda_m \mu_e$, leading to the outcome where $A = 1$ and $B = 0$. In contrast, set 2 and set 3 exhibit deviations from each other and from the classical theory at various radial positions. This comparison highlights the influence of different parameter sets on the radial displacement.

Table 1: Values of the parameters of the relaxed micromorphic model

Set	λ_M (GPa)	μ_M (GPa)	λ_m (GPa)	μ_m (GPa)	Ref.
1	17.61	16.13	30.82	28.23	[36]
2	1.75	5.90	11.30	10.19	[35]
3	1.75	5.90	8.22	10.55	[35]

To illustrate the effect of the characteristic length, Figures 3 and 4 show the variations of the non-dimensional parameter δ , defined by $(u_r)_{\text{Micro.}} - (u_r)_{\text{Class.}}/U_0$, as a function of radial position. These figures compare the cases where $L_c \rightarrow \infty$ and $L_c \rightarrow 0$ for the parameters of set 3. As expected, the characteristic length influences the displacement profile. It is observed that when the characteristic length is either very large $L_c \rightarrow \infty$ or very small $L_c \rightarrow 0$, the displacement profile of the relaxed micromorphic model effectively reduces to the classical model, indicating minimal impact from the microstructure. Furthermore, the results reveal that the relaxed micromorphic model predicts a smaller displacement than the classical model at certain radial positions. This behavior highlights the critical importance of considering characteristic length in material design and analysis, as it directly influences the accuracy of displacement predictions and the overall performance of the material.

Furthermore, to illustrate the effects of λ_m and μ_m , Figures 5 and 6 present the variations of the parameter δ as a function of radial position. In Figure 5, the parameters are set as $\lambda_M = 1.75$, $\mu_M = 5.9$, $\mu_m = 10.55$, and $R/L_c = 5$, with $\lambda_m = \beta_1 \lambda_M$. Similarly, in Figure 6, the parameters are $\lambda_M = 1.75$, $\mu_M = 5.9$, $\lambda_m = 8.22$, and $R/L_c = 5$, with $\mu_m = \beta_2 \mu_M$. It is observed that, for $\beta_1 < 2$, the relaxed micromorphic model predicts a lower displacement than the classical model. Conversely, for $\beta_1 > 2$, the behavior contrasts, indicating a complex interaction between the microstructural parameters and the overall displacement response. These findings emphasize the importance of parameter selection in the relaxed micromorphic model. Furthermore, it is observed that with increasing β_2 the relaxed micromorphic model reduces to the classical model.

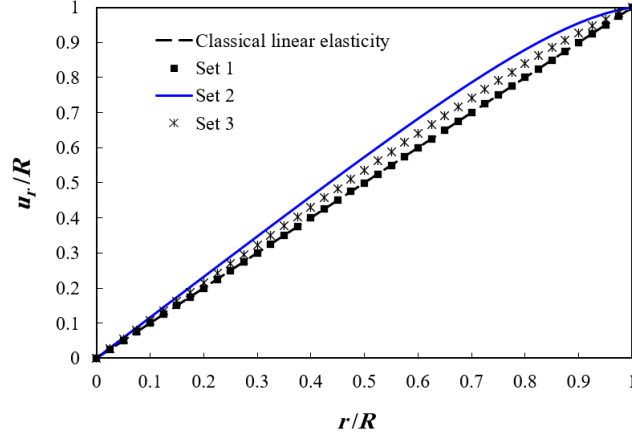


Figure 2: Profile of non-dimensional radial displacement for classical elasticity and the relaxed micromorphic model for three parameter sets and $R/L_c = 2$.

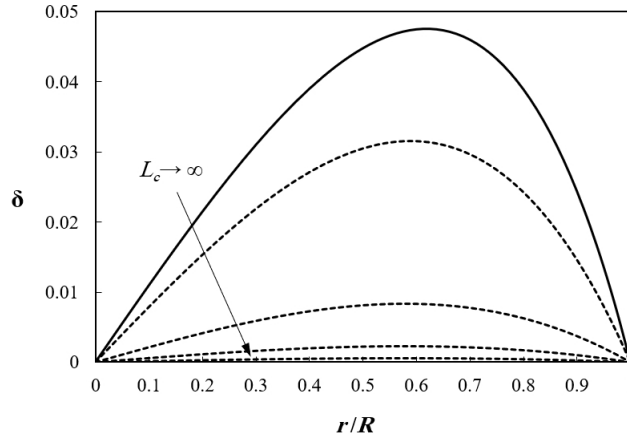


Figure 3: Comparison between the relaxed micromorphic and the classical models for $R/L_c = \{0.05, 0.1, 0.2, 0.5, 1\}$.

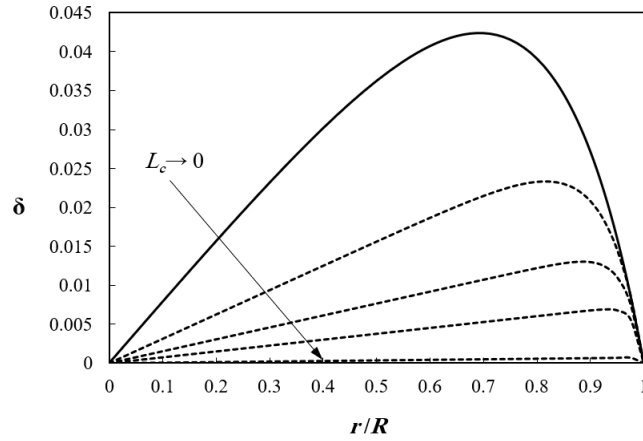


Figure 4: Comparison between the relaxed micromorphic and the classical models for $R/L_c = \{2, 5, 10, 20, 200\}$.

5 Conclusions

In this paper, we have successfully derived the governing equations of the isotropic relaxed micromorphic model in polar coordinates and then used the relations to solve an elastostatic axisymmetric extension problem. By utilizing modified Bessel functions, we derived closed-form solutions for both displacement and microdistortion fields using the consistent coupling boundary conditions. Our analysis demonstrated that the relaxed micromorphic model effectively captures size-dependent behaviors, which are not accounted for by classical continuum theories.

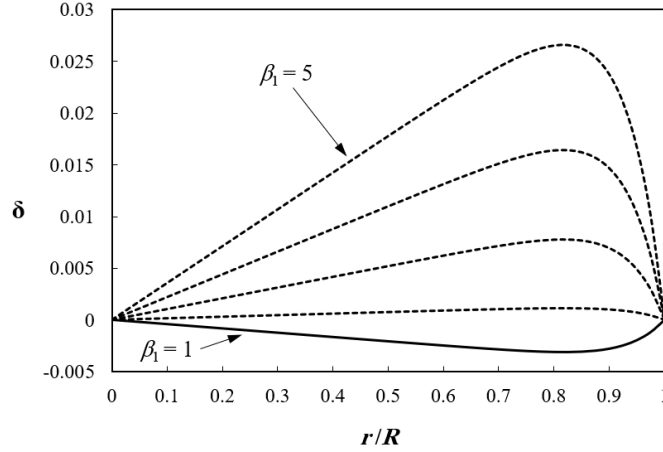


Figure 5: Variations of parameter δ as a function of radial position for $\beta_1 = \{1, 2, 3, 4, 5\}$.

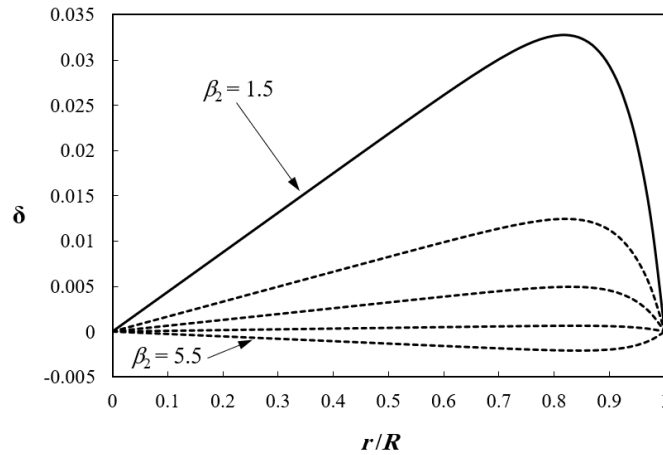


Figure 6: Variations of parameter δ as a function of radial position for $\beta_2 = \{1.5, 2.5, 3.5, 4.5, 5.5\}$.

Furthermore, we showed that the classical linear elasticity model can be obtained as limit-cases of the relaxed micromorphic model, highlighting its versatility and robustness. The numerical results provided insights into the effects of various parameters, such as the characteristic length and material coefficients, on the displacement. These findings underscore the importance of considering microstructural effects in material modeling to achieve accurate predictions of mechanical behavior.

Acknowledgement

The authors are grateful to P. Gourgiotis (National Technical University of Athens), A. Sky (University of Luxembourg) and M. Sarhil (Technical University Dortmund) for critical proof reading and helpful remarks.

References

- [1] S. Alavi, J. Ganghoffer, H. Reda, and M. Sadighi. “Hierarchy of generalized continua issued from micromorphic medium constructed by homogenization”. *Continuum Mechanics and Thermodynamics* 35.6 (2023), 2163–2192.
- [2] R. Alberdi, J. Robbins, T. Walsh, and R. Dingreville. “Exploring wave propagation in heterogeneous metastructures using the relaxed micromorphic model”. *Journal of the Mechanics and Physics of Solids* 155 (2021), 104540.
- [3] H. Askes and E. C. Aifantis. “Gradient elasticity in statics and dynamics: an overview of formulations, length scale identification procedures, finite element implementations and new results”. *International Journal of Solids and Structures* 48.13 (2011), 1962–1990.
- [4] G. Barbagallo, A. Madeo, M. V. d’Agostino, R. Abreu, I.-D. Ghiba, and P. Neff. “Transparent anisotropy for the relaxed micromorphic model: macroscopic consistency conditions and long wave length asymptotics”. *International Journal of Solids and Structures* 120 (2017), 7–30.

- [5] J. L. Bleustein. “Effects of micro-structure on the stress concentration at a spherical cavity”. *International Journal of Solids and Structures* 2.1 (1966), 83–104.
- [6] H. Cui, R. Hensleigh, H. Chen, and X. Zheng. “Additive manufacturing and size-dependent mechanical properties of three-dimensional microarchitected, high-temperature ceramic metamaterials”. *Journal of Materials Research* 33.3 (2018), 360–371.
- [7] M. V. d’Agostino, G. Rizzi, H. Khan, P. Lewintan, A. Madeo, and P. Neff. “The consistent coupling boundary condition for the classical micromorphic model: existence, uniqueness and interpretation of parameters”. *Continuum Mechanics and Thermodynamics* 34.6 (2022), 1393–1431.
- [8] P. Demetriou, G. Rizzi, and A. Madeo. “Reduced relaxed micromorphic modeling of harmonically loaded metamaterial plates: investigating boundary effects in finite-size structures”. *Archive of Applied Mechanics* 94.1 (2024), 81–98.
- [9] A. C. Eringen. *Microcontinuum Field Theories. I. Foundations and Solids*. Springer-Verlag New York, 1999.
- [10] S. Forest and R. Sievert. “Nonlinear microstrain theories”. *International journal of solids and structures* 43.24 (2006), 7224–7245.
- [11] E. Ghavanloo, S. A. Fazelzadeh, and F. Marotti de Sciarra. *Size-Dependent Continuum Mechanics Approaches*. Springer, 2021.
- [12] F. Gmeineder, P. Lewintan, and P. Neff. “Korn-Maxwell-Sobolev inequalities for general incompatibilities”. *Mathematical Models and Methods in Applied Sciences* 34.3 (2024), 523–570.
- [13] F. Gmeineder, P. Lewintan, and P. Neff. “Optimal incompatible Korn–Maxwell–Sobolev inequalities in all dimensions”. *Calculus of Variations and Partial Differential Equations* 62.6 (2023), 182.
- [14] P. Gourgiotis, G. Rizzi, P. Lewintan, D. Bernardini, A. Sky, A. Madeo, and P. Neff. “Green’s functions for the isotropic planar relaxed micromorphic model—Concentrated force and concentrated couple”. *International Journal of Solids and Structures* 292 (2024), 112700.
- [15] X. Ju, K. Gao, J. Huang, H. Ruan, H. Chen, Y. Xu, and L. Liang. “A three-dimensional computational multiscale micromorphic analysis of porous materials in linear elasticity”. *Archive of Applied Mechanics* 94.4 (2024), 819–840.
- [16] D. Knees, S. Owczarek, and P. Neff. “Global regularity for a physically nonlinear version of the relaxed micromorphic model on Lipschitz domains”. *arXiv preprint arXiv:2403.17451, to appear in Calculus of Variations and Partial Differential Equations* (2025).
- [17] R. Lakes. “Cosserat shape effects in the bending of foams”. *Mechanics of Advanced Materials and Structures* 30.19 (2023), 3997–4001.
- [18] P. Lewintan, S. Müller, and P. Neff. “Korn inequalities for incompatible tensor fields in three space dimensions with conformally invariant dislocation energy”. *Calculus of Variations and Partial Differential Equations* 60 (2021), 1–46.
- [19] J. Liu, R. Papadakis, and H. Li. “Experimental observation of size-dependent behavior in surface energy of gold nanoparticles through atomic force microscope”. *Applied Physics Letters* 113.8 (2018).
- [20] A. Madeo, P. Neff, M. V. d’Agostino, and G. Barbagallo. “Complete band gaps including non-local effects occur only in the relaxed micromorphic model”. *Comptes Rendus Mécanique* 344.11-12 (2016), 784–796.
- [21] A. Madeo, P. Neff, I.-D. Ghiba, L. Placidi, and G. Rosi. “Band gaps in the relaxed linear micromorphic continuum”. *Zeitschrift für Angewandte Mathematik und Mechanik* 95.9 (2015), 880–887.
- [22] R. D. Mindlin. “Micro-structure in linear elasticity”. *Archive for Rational Mechanics and Analysis* 16 (1964), 51–78.
- [23] P. Neff and S. Forest. “A geometrically exact micromorphic model for elastic metallic foams accounting for affine microstructure. Modelling, existence of minimizers, identification of moduli and computational results”. *Journal of Elasticity* 87.2 (2007), 239–276.
- [24] P. Neff, I.-D. Ghiba, A. Madeo, L. Placidi, and G. Rosi. “A unifying perspective: the relaxed linear micromorphic continuum”. *Continuum Mechanics and Thermodynamics* 26 (2014), 639–681.
- [25] P. Neff, D. Pauly, and K.-J. Witsch. “Poincaré meets Korn via Maxwell: extending Korn’s first inequality to incompatible tensor fields”. *Journal of Differential Equations* 258.4 (2015), 1267–1302.
- [26] S. Owczarek, I.-D. Ghiba, and P. Neff. “A note on local higher regularity in the dynamic linear relaxed micromorphic model”. *Mathematical Methods in the Applied Sciences* 44.18 (2021), 13855–13865.
- [27] E. Papamichos. “Continua with microstructure: Cosserat theory”. *European Journal of Environmental and Civil Engineering* 14.8-9 (2010), 1011–1029.
- [28] E. Pouramiri and E. Ghavanloo. “Estimation of effective bulk modulus of metamaterial composites with coated spheres using a reduced micromorphic model”. *Iranian Journal of Science and Technology, Transactions of Mechanical Engineering* (2024), <https://doi.org/10.1007/s40997-024-00799-2>.
- [29] J. N. Reddy. *An Introduction to Continuum Mechanics*. Cambridge University Press, 2013.
- [30] G. Rizzi, G. Hütter, H. Khan, I.-D. Ghiba, A. Madeo, and P. Neff. “Analytical solution of the cylindrical torsion problem for the relaxed micromorphic continuum and other generalized continua (including full derivations)”. *Mathematics and Mechanics of Solids* 27.3 (2022), 507–553.
- [31] G. Rizzi, G. Hütter, A. Madeo, and P. Neff. “Analytical solutions of the cylindrical bending problem for the relaxed micromorphic continuum and other generalized continua”. *Continuum Mechanics and Thermodynamics* 33 (2021), 1505–1539.
- [32] G. Rizzi, H. Khan, I.-D. Ghiba, A. Madeo, and P. Neff. “Analytical solution of the uniaxial extension problem for the relaxed micromorphic continuum and other generalized continua (including full derivations)”. *Archive of Applied Mechanics* (2021), 1–17.
- [33] G. Romano, R. Barretta, and M. Diaco. “Micromorphic continua: non-redundant formulations”. *Continuum Mechanics and Thermodynamics* 28 (2016), 1659–1670.
- [34] M. H. Sadd. *Elasticity: Theory, Applications, and Numerics*. Academic Press, 2009.

- [35] M. Sarhil, L. Scheunemann, P. Lewintan, J. Schröder, and P. Neff. “A computational approach to identify the material parameters of the relaxed micromorphic model”. *Computer Methods in Applied Mechanics and Engineering* 425 (2024), 116944.
- [36] M. Sarhil, L. Scheunemann, J. Schröder, and P. Neff. “Size-effects of metamaterial beams subjected to pure bending: on boundary conditions and parameter identification in the relaxed micromorphic model”. *Computational Mechanics* 72.5 (2023), 1091–1113.
- [37] J. Schröder, M. Sarhil, L. Scheunemann, and P. Neff. “Lagrange and $H(\text{curl},B)$ based finite element formulations for the relaxed micromorphic model”. *Computational Mechanics* 70.6 (2022), 1309–1333.
- [38] M. Shaat. “A reduced micromorphic model for multiscale materials and its applications in wave propagation”. *Composite Structures* 201 (2018), 446–454.
- [39] A. Sky, M. Neunteufel, P. Lewintan, A. Zilian, and P. Neff. “Novel $H(\text{symCurl})$ -conforming finite elements for the relaxed micromorphic sequence”. *Computer Methods in Applied Mechanics and Engineering* 418 (2024), 116494.
- [40] A. Sky, M. Neunteufel, I. Muench, J. Schöberl, and P. Neff. “Primal and mixed finite element formulations for the relaxed micromorphic model”. *Computer Methods in Applied Mechanics and Engineering* 399 (2022), 115298.
- [41] C. Xiu, X. Chu, J. Wang, W. Wu, and Q. Duan. “A micromechanics-based micromorphic model for granular materials and prediction on dispersion behaviors”. *Granular Matter* 22 (2020), 1–22.
- [42] G. Zhang, X.-L. Gao, C. Zheng, and C. Mi. “A non-classical Bernoulli-Euler beam model based on a simplified micromorphic elasticity theory”. *Mechanics of Materials* 161 (2021), 103967.